Neutralization of He^+ ions in front of an aluminum surface

B. van Someren, P. A. Zeijlmans van Emmichoven, and A. Niehaus
Debye Institute, Utrecht University, Princetonplein 5, 3584 CC Utrecht, The Netherlands
(Received 14 July 1999; published 10 January 2000)

We report electron spectra obtained from grazing incidence collisions of He^+ ions with an Al(111) surface at collision energies ranging from 200 eV up to a few keV. The part of the spectra due to potential electron emission is analyzed in terms of a rate equation model that uses transition rate constants for resonant charge exchange– and Auger-type processes, and interaction energies between the projectile and the surface. It is shown that, if recently obtained theoretical interaction energies and rate constants are used in the model, calculated and experimental electron spectra agree within experimental error. From this it is concluded that (i) the theoretical input information on the He/Al system is consistent with experiment and (ii) the rate equation model is a valuable tool for analyzing electron spectra.

PACS number(s): 79.20.Rf, 79.20.Ap

INTRODUCTION

When ions slowly approach a metal surface, two different types of processes can occur: (i) resonant transitions (RT) of one electron, i.e., resonant capture (RC), and resonant ionization (RI); and (ii) Auger-type two-electron processes that lead to ejection of an electron (see, e.g., [1]). The latter processes are called Auger capture (AC) processes if two metal electrons are involved, and Auger deexcitation (AD) processes if one metal electron and one atomic electron are involved. We consider here ''grazing incidence'' collisions, where the perpendicular energy $E_{\mathrm{col}}\sin^2(\vartheta)$ is of the order of 1 eV or less, so that the projectile trajectory lies outside the first surface layer and is essentially independent on the impact point at the surface. In the case of He^+ ions approaching an Al(111) surface (M) along such trajectories, the scheme of possible processes that can occur is rather simple:

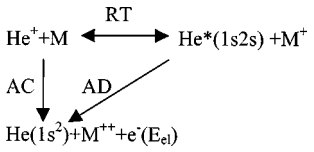

(1)

A scheme of processes like Eq. (1) implies a certain time evolution of the system during the collision. Since the DeBroglie wave length corresponding to the perpendicular energies is small compared to the length of the trajectories in the interaction region, this time evolution can be described in terms of transition rates and population probabilities along the classical trajectories. A general difficulty that arises in such a description is due to the fact that the forces determining the trajectories depend on the projectile state, so that an initially well-defined trajectory branches into many individual trajectories, depending on the time points of transitions between the states involved. An approximate way, which simplifies a description of the time evolution considerably, implies the assumption that a well-defined one-dimensional trajectory $z(t)$ may be defined. In that case the evolution of the system can be described by a set of coupled rate equations for the population probabilities of the projectile states involved, and electron spectra can be obtained from the population probabilities of those states that decay irreversibly by electron emission. The calculation of electron spectra by itself is of course still far from trivial and requires, in addition to the total z-dependent ionization rates, (i) the interaction potentials for the initial and final state of the projectile, and (ii), an approximate decomposition of the total ionization rate into the differential rates for defined initial and final electronic states of the metal [1,2].

The rate equation description sketched above has been applied frequently in the past to the qualitative analysis of electron spectra. In the absence of sufficient theoretical information, model functions for both the transition rates and the interaction potentials were used, and the Auger-type transitions were described in terms of the unperturbed surface density of electronic states (SDOS) [1–8]. It has been shown that experimental electron spectra could very well be reproduced qualitatively in this way, leading to an identification of the features observed in the electron spectra and to an approximate reconstruction of the time evolution of the projectile-surface system—even for cases of rather complicated reaction schemes [2–8]. As an implicit result of these analyses, the reaction rate constants involved in the reaction schemes were determined while the interaction energies were estimated. Due to the uncertainties implied in these estimates, such semiempirically obtained rate constants have to be considered as uncertain, to an extent depending on the system.

In the case of the He^+/Al(111) system, recently sufficient theoretical information has become available to calculate electron spectra within the rate equation model, and to compare the result with measured electron spectra. Such a comparison is the main purpose of the present work.

EXPERIMENT AND EXPERIMENTAL RESULTS

A mass selected He^+ beam is directed at a single-crystal Al(111) surface mounted on a manipulator. The polar and azimuth angles of incidence (ϑ) and (ϕ), respectively, with (ϑ) defined relative to the surface, are controlled by rotating the manipulator with an accuracy of ca. 0.1°. The crystal surface is prepared by sputter cleaning and annealing, and its

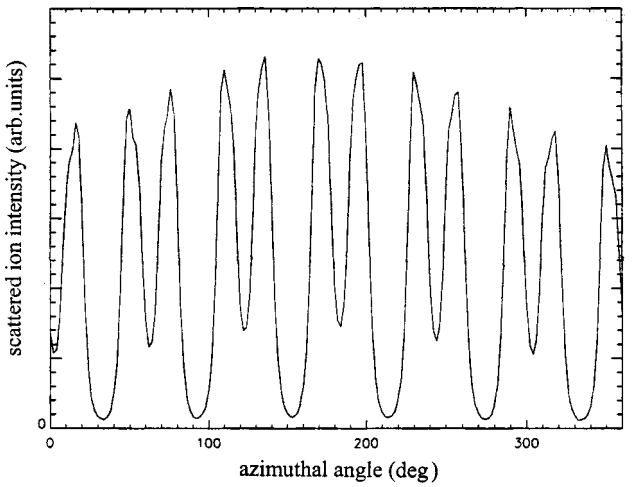

FIG. 1. Scattered ion intensity plotted as a function of the azimuthal angle of incidence for 1-keV He^+ ions at 8° grazing angle incident on Al(111). The ions are measured in the direction of the surface normal. Low intensity indicates the absence of hard collisions, i.e., ''grazing conditions.'' Such conditions are realized in the direction of the ''closest packed'' surface directions.

quality is controlled by low-energy ion scattering (LEIS) [see, e.g., [9]]. Especially, the realization of ''grazing conditions'' was tested by monitoring large-angle scattering of He^+ at small polar incidence angles. An example of an azimuth scan for $\vartheta = 8°$ incidence angle at an energy of 1 keV and 90° scattering is shown in Fig. 1. Note that ''grazing conditions,'' i.e., the absence of hard binary collisions of He with the individual surface atoms, and hence near specular deflection of the incident beam, is realized in the six closest packed surface directions of the sixfold rotational symmetry of the (111) surface of the Al fcc crystal. Upon decreasing the incidence angle further, grazing conditions are realized successively also for the other directions. The electron spectra to be discussed in this paper are measured for $\vartheta = 2°$ along one of the closest-packed directions. Before and after each measurement the realization of grazing conditions was monitored. The electrons emitted as a result of the He^+-Al(111) interaction are detected by a hemispherical electrostatic analyzer in a direction perpendicular to the surface. The analyzer has an energy resolution of ca. 3% and accepts ca. 10^{-4} sr. We measured electron spectra for collision energies ranging from 0.2 to 5.0 keV. While at 0.2 keV virtually no kinetic emission occurs, the contribution of kinetic emission to the spectra becomes appreciable at the higher collision energies. Since we want to analyze the spontaneous ionization processes, we subtract the contributions due to kinetic emission from the spectra. This can be done in a rather straightforward way because the kinetic part has approximately the form of an exponential that extends beyond the energy region of the spontaneous-emission part and can therefore be determined in that region.

The spontaneous emission spectra obtained in the described way are reproduced in Fig. 2 for the three collision energies 0.2, 0.5, and 1.0 keV. The electron-energy scale has been calibrated experimentally with an accuracy of better than 0.5 eV, and the spectra are corrected for the transmission function of the spectrometer. Below an energy of approximately 5 eV, the transmission function is unreliably known due to imperfect compensation of the earth's magnetic field, and the spectra are not shown in that region.

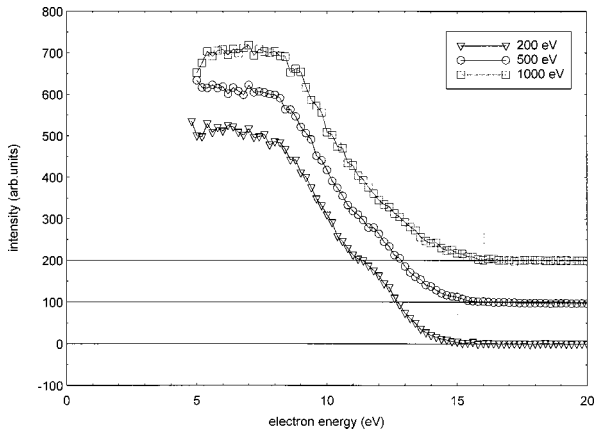

FIG. 2. Measured spontaneous emission electron spectra for He^+/Al(111) at 2° grazing incidence angle and three different kinetic energies. Below ca. 5 eV electron energy the spectra are not reliable due to stray magnetic fields. The spectra are normalized in intensity and shifted by 100 arb. unit for clarity.

CALCULATION OF ELECTRON SPECTRA

For a calculation of the electron spectra within the rate equation description sketched in the Introduction, we need the interaction potentials for He in the states $He^+(1s)$, $He^*(2\ ^3S)$, and $He(1s^2)$ with the Al surface. For $He^+(1s)$ and $He(1s^2)$, these potentials have been calculated by Merino *et al.* [10] using an ''LCAO [linear combination of atomic orbitals] method supplemented with a LD many-body contribution.'' These authors report calculated points at distances from 1 to 7 a.u. outside the first atomic layer, 1 a.u. apart. It turns out that this distance region covers the region most relevant for Auger neutralization, so that an extrapolation of the potential to smaller and larger distances does not introduce significant uncertainties. The extrapolated He^+ potential is made to approach asymptotically the image-charge interaction $[-1/(4z)]$ with the image plane position taken to be 3 a.u. in front of the first atom layer. This value of 3 a.u. is the sum of the ''jellium edge''–surface distance of 2.2 a.u. for Al and the image plane-''jellium edge'' distance of 0.8 a.u. [11]. For $He(2\ ^3S)$-Al, no theoretical interaction potential is available. However, Dunning *et al.* [12] have calculated the $He^*(2\ ^3S)$-Cu interaction potential. Since they treated the Cu as a ''jellium,'' their potential is probably also a reasonable approximation for the $He(2\ ^3S)$-Al potential. We will use this potential in our model. It is defined relative to the jellium edge. In order to use it in our calculation we therefore shift it by the jellium edge–image plane distance of 0.8 a.u.

The potentials obtained in this way are shown in Fig. 3 in a diagram that allows one to visualize the processes of scheme 1. This is done by normalizing the potentials as follows:

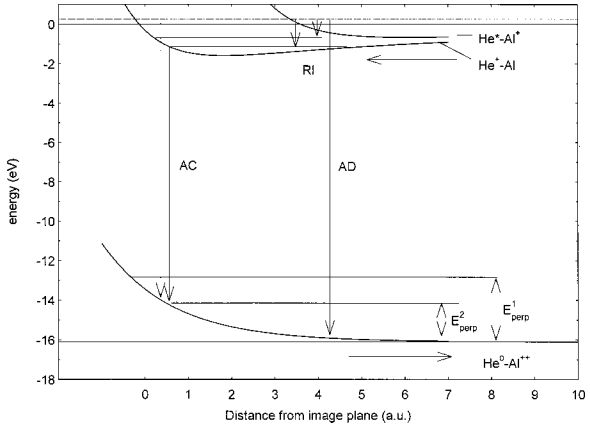

FIG. 3. Potentials used in the model calculations. The potentials are normalized to the total asymptotic energy of the He-metal system involving the respective atomic states and the respective ground state of the metal. The arrows indicate the possible electronic transitions, resonant ionization RI, Auger deexcitation AD, and Auger capture AC. Also indicated are the final perpendicular kinetic energies resulting from direct AC (E^1_{perp}), and ''indirect AC'' (E^2_{perp}).

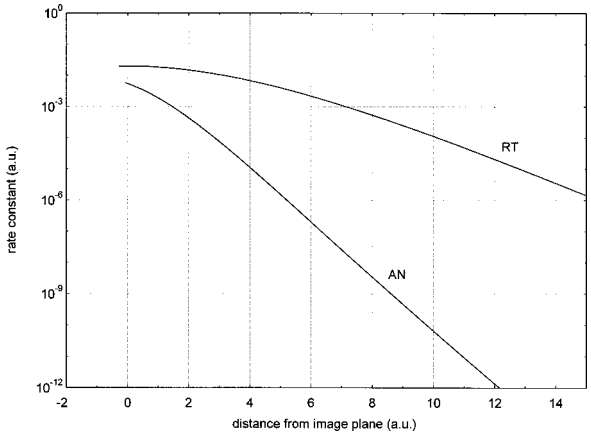

FIG. 4. Theoretical rate constants used in the model calculations. The Auger neutralization (AN) rate constant is adapted from Ref. [13], and the resonant transition (RT) rate constant is adapted from Ref. [12].

(i) The He^+-Al potential is set to zero energy asymptotically.

(ii) The He^0-Al^{2+} potential is shifted to an asymptotic energy of $E(\infty) = -IP(\mathrm{He}) + 2\Phi = -16.1\,\mathrm{eV}$.

(iii) The He*($2\,^3S$)-Al^+ potential is shifted to an asymptotic energy of $E(\infty) = -IP(\mathrm{He}^*) + \Phi = -0.55\,\mathrm{eV}$.

Here $\Phi = 4.25\,\mathrm{eV}$ is the work function of Al, $IP(\mathrm{He}) = 24.6\,\mathrm{eV}$ the ionization energy of He, and $IP(\mathrm{He}^*(2\,^3S)) = 4.8\,\mathrm{eV}$ the ionization energy of He($2\,^3S$). The electron energies for AC and AD transitions involving one or two electrons from the Fermi-level, respectively, are then simply given by the vertical energy separation between the potentials at the transition distance. If electrons from below the Fermi level are involved, correspondingly lower electron energies result from the transitions. Resonant charge-transfer transitions may be visualized in the diagram by vertical transitions between the He^+-Al potential and the He*-Al^+ potential. These two potentials cross at a distance of 12.5 a.u., where the He*($2\,^3S$) level crosses the Fermi level. Therefore, at distances smaller than 12.5 a.u., RC transitions correspond to capture of a metal electron from occupied states above the Fermi level, and RI transitions correspond to loss of an atomic electron into empty metal states above the Fermi level. The electronic energies implied in these transitions are, respectively, gained from the parallel motion via the Doppler shift in case of RC, and lost to the metal via electronic relaxation in case of RN. For all electronic transitions, it is assumed, as usual, that the instantaneous perpendicular kinetic energy of the projectile is conserved. We notice that neutralization to the ground state of the atom can occur (1) directly by the AC process, (2) indirectly by the AC process after intermediate resonant capture and loss of an electron, and (3) by the AD process from the metastable state after resonant capture of an electron. The final perpendicular kinetic energy can be drastically different for the different processes. Especially, indirect AC neutralization will generally lead to significantly lower final kinetic energies than direct AC neutralization, because in the indirect process the projectile will be retarded in the He*-Al^+ potential, so that, after RI, it will have a lower kinetic energy when it gets neutralized in the AC process. Since the kinetic energy is conserved in the AC transition, this leads to a lower perpendicular energy. This is also indicated in the diagram.

The other crucial quantities we need are the rate constants for Auger transitions to the ground state. The total rate constant for the He^+/Al system, including both AD and AC processes and in addition a plasmon-assisted Auger decay, has recently been calculated by Lorente and Monreal [13], using a ''self-consistent LDA [local density approximation] method.'' Later, more refined calculations of the same total rate constant by Cazalilla *et al.* [14] have been published, in which the perturbation of the surface by the ion is more explicitly taken into account. Although this total rate constant is not exactly the theoretical input information needed in our reaction scheme, where AC and AD are distinguished and where plasmon-assisted decay is not explicitly taken into account in calculating the shape of the electron spectra, we will use this rate constant. In fact, the total neutralization will be described appropriately in this way, and a certain ambiguity only arises in calculating the shape of the electron spectra. We will see that, for the final comparison of experimental and calculated electron spectra, this ambiguity is not important. The theoretical rate constant of Ref. [13] is reproduced in Fig. 4. The rate constant of the refined calculations [14] is about a factor of 5 larger and has a similar distance dependence.

Finally, we need the rate constants for the resonant electron exchange processes. Here, a problem arises because of the rather swift motion of the atomic particles parallel to the surface. Even if a transition rate $\Gamma_0(z)$, as calculated for fixed distances (z), is available, the rate function $\Gamma(z,v)$ to be used in the rate equations depends very sensitively on the relative velocity (v), because the actual rate has to account for the availability of ''empty metal states'' in the case of RI,

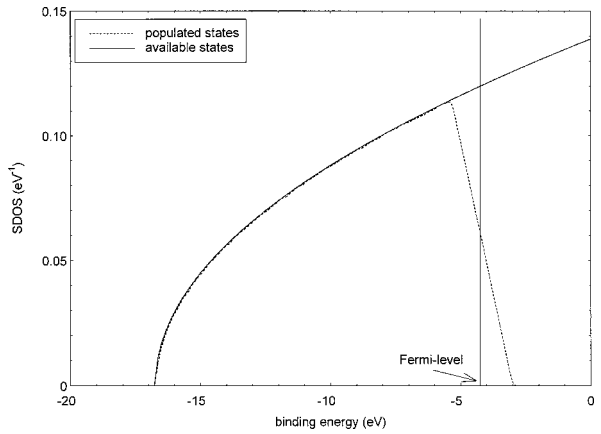

FIG. 5. The SDOS function used in the calculations. It arises from the ''jellium'' SDOS of aluminum by a Galilei transformation for a relative velocity corresponding to a collision of He at an energy of 200 eV.

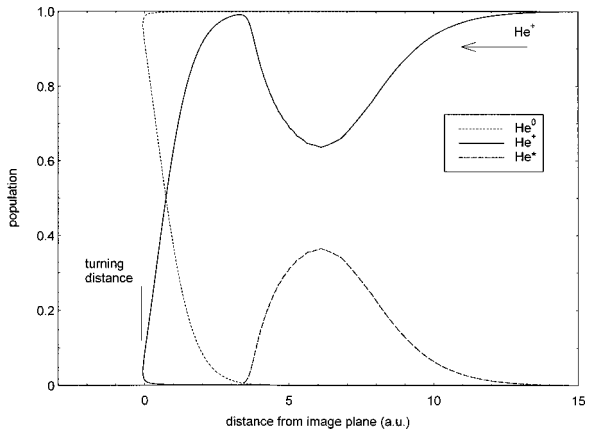

FIG. 6. The population of the states distinguished in the neutralization scheme (1), calculated for a grazing incidence collision of He^+ at 2° and 200 eV.

and of ''populated metal states'' in the case of RC. Within the ''jellium model'' for a metal, it is customary to take the influence of the parallel motion approximately into account by a Galilei transformation of the Fermi sphere of velocities of the free metal electrons (see, e.g., [15]). This leads to a density-of-states function that decreases gradually from ''fully occupied'' to ''zero'' across the Fermi level. For the case of He at 200 eV of kinetic energy, the resulting transformed surface density of electronic states (SDOS) is shown in Fig. 5. The relative energy position of the Fermi level with respect to the atomic level is given by the potential curves (see Fig. 3): if the population of metal states would change stepwise at the Fermi level, RC would only be possible outside the crossing distance at 12.5 a.u., and RI only inside, whereas in case of the transformed SDOS a rather wide region exists where both RC and RI occur simultaneously. Especially, RC is possible in the dynamical situation down to rather small distances, leading to significant populations of the He($2\ ^3S$) state close to the surface. Within the rate equation model, the actual rates are constructed as

$$\Gamma_{\mathrm{RC}}(z,v)=\Gamma_0(z)N_p(z,v) \quad \text{for RC,} \tag{2a}$$

$$\Gamma_{\mathrm{RI}}(z,v)=\Gamma_0(z)N_e(z,v) \quad \text{for RI,} \tag{2b}$$

where N_p and N_e are the branching ratios for populated and empty states, respectively. These branching ratios depend sensitively on the parallel velocity, and result directly from the transformed SDOS at a given distance from the surface.

A velocity-independent rate constant $\Gamma_0(z)$ for resonance transitions that could directly be used to define the velocity-dependent rate constants by relations (2a) and (2b) has been reported for the He^+-Cu system [12]. It is obtained in calculations treating the Cu as a ''jellium,'' and may therefore also be used as an approximation for the He^+-Al case. It is given as a function of the distance from the ''jellium edge.'' In order to use it in our model, we shift it by the jellium edge–image plane distance of 0.8 a.u. The resulting rate constant is shown in Fig. 4.

In Fig. 6 we show the populations resulting from the solution of the rate equations using the rate constant for resonant charge transfer of Ref. [12] and the Auger neutralization rate constant of Ref. [13]. The calculations refer to a collision energy of 200 eV and an incidence angle of 2°. We notice that most of the Auger transitions leading to neutral He in the ground state occur rather close to the turning point, in a narrow region centered at 0.5 a.u. in front of the image plane. Projectiles that have been neutralized at intermediate distances lose their electron before they reach distances where Auger transitions become significant, so that the AD process is unimportant.

With the populations determined in this way, the electron spectra are calculated using the method described in our earlier publications (e.g., [2,3,5,8]). In these calculations, Galilei-transformed SDOS functions, as shown in Fig. 5 for a collision energy of 200 eV, and the potentials shown in Fig. 3, are used. The resulting electron spectra are compared with the experimental spectra in Fig. 7. Since the experimental spectra are not on an absolute scale, the spectra are normalized with respect to each other in intensity for each collision energy. We notice good agreement between calculated and measured spectral shapes. The observed slight structure in

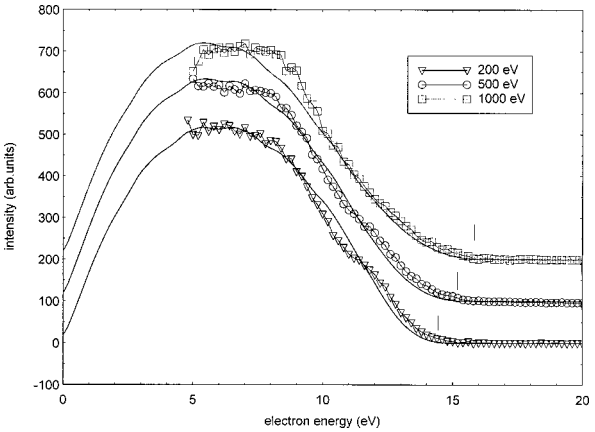

FIG. 7. Comparison of calculated and measured electron spectra arising from spontaneous electron emission for grazing incidence He^+ collisions at 2° and three different collision energies.

the high-energy flank, best visible in the 200-eV spectrum, is not reproduced. It could be due to plasmon excitation [13] or to structure in the SDOS caused by the ion-surface interaction at the rather small distances involved [14,16]. Noteworthy is the very good agreement of the high-energy onset of the spectra and of its variation with collision energy. This onset is caused by Auger transitions involving two electrons from the Fermi level, and its energy position in the calculated spectra is on the one hand rather independent of the method used for the calculations, but on the other hand very sensitive to the potentials and the rates used.

DISCUSSION

The good agreement suggests that the theoretical input used to calculate the spectra is approximately correct. It is difficult to say *how* correct, because of the interconnectedness of the potentials and rate constants. One therefore might prefer to state that the theoretical input is *consistent* with the experimental results.

As already mentioned above, the onset of the spectra, involving two electrons from the Fermi level, are rather sensitive to the initial- and final-state potentials. For instance, calculations show that an outward shift of the final-state potential by 0.5 a.u. leads to an energy shift of the onset by about 1 eV, which would be clearly visible in the measurement. On the other hand, since the energy separation between initial and final state of the AC process happens to vary rather little in the transition region, the electron spectra are not very sensitive to the absolute AC transition rate constant. We have carried out calculations using the five times higher Auger neutralization rate constant of Ref. [14] and found that such a higher rate constant is still consistent with the observed spectra, although the transition region shifts outward by about 1 a.u.

It is interesting to discuss, in the light of the present analysis, recently published angular distributions of backscattered neutralized He in grazing ($\vartheta = 0.5°$) incidence collisions of He^+ on Al(111) at 2000 eV [17]. The exit angles in such an experiment are closely related with the electron spectra. In fact, if specular reflection prevails, the exit angles are simply determined by the final perpendicular kinetic energy corresponding to an AC transition at a certain distance. For small scattering angles (Θ) we have the approximate relations,

$$\Theta = \vartheta_{\mathrm{inc}} + \vartheta_{\mathrm{exit}}, \quad \vartheta_{\mathrm{exit}}[\mathrm{rad}] = [E_{\mathrm{perp}}/E_{\mathrm{beam}}]^{1/2}. \qquad (3)$$

The perpendicular energies of the neutralized He projectiles that arise according to the present analysis can simply be read off the potential curve diagram (see Fig. 3). We notice that direct AC processes that occur within the main transition region around 0.5 a.u. in front of the image plane lead to final perpendicular energies of about $E^1_{\mathrm{perp}} = 3$ eV. This energy results partly from acceleration in the initial He^+-Al potential and partly from repulsion in the final He^0-Al^{2+} potential. According to Eq. (3), the corresponding exit angle is $\vartheta_{\mathrm{exit}} = 2.2°$ if a beam energy of 2000 eV is assumed. In the case of the indirect AC process, the projectile is retarded in the He*-Al^+ potential, and the RI transitions, which occur mainly close to the turning point on that potential, lead to low local kinetic energies in the AC transition region. As indicated in Fig. 3, the resulting final perpendicular energy is smaller by about 1 eV, leading to a value of $E^2_{\mathrm{perp}} = 2$ eV, and via relation (3), to an exit angle of $\vartheta_{\mathrm{exit}} = 1.8°$. Since the incident perpendicular energy of $E_{\mathrm{perp}} = 2000\,[0018]\sin^2\vartheta = 0.15$ eV in the experiment of Ref. [17] is very similar to the value of $E_{\mathrm{perp}} = 200\sin^2\vartheta = 0.25$ eV, used for the calculations of the populations (see Fig. 6) and in the potential curve diagram, the estimated angles should also be good estimates of the exit angles the present analysis predicts for the experiment of Ref. [17]. What is actually measured is a slightly asymmetric distribution of exit angles that extends from 1° to 2.5°, with a maximum at 2° and a shoulder around 1.7°; in other words, a distribution that is expected on the basis of the above estimate. We conclude from this that our analysis is consistent with the experimental angular distributions of Ref. [17].

Although, as shown above, the measured angular distributions are consistent with our electron spectra, as well as with the theoretical input used in our analysis, the semiempirical Auger rate constant that was retrieved from the angular distributions is higher, by about two orders of magnitude in the relevant distance region, than the theoretical rate constant used in our analysis. This dramatic disagreement was already pointed out in Ref. [17] and was ascribed to deficiencies of the theoretical methods applied in calculating the rate constant. From our analysis, it is quite clear, however, that, if the angular distributions would have been analyzed using the theoretical potentials used in our analysis, the rate constant obtained could not have been in significant disagreement with the theoretical one. In other words, there is no disagreement between experiment and theory.

There is a simple reason why the rate constant retrieved in Ref. [17] from the angular distributions is so different. It was *assumed* in the analysis that the neutralizing transitions would occur at sufficiently large distances from the surface to allow one to use a pure image potential $[-1/(4z)]$ for the initial state of the AC process and a constant potential for the final state. In this assumed scenario, the final perpendicular kinetic energy necessarily has to be due purely to acceleration in the *attractive image potential in the initial state*, and the observed small average exit angle of 2° leads necessarily to a correspondingly high neutralization rate that achieves neutralization at sufficiently large distances of about 3 a.u. in front of the image plane.

Obviously, the angular distribution experiment can be explained in the two rather different scenarios, and is consistent with the two corresponding very different AC rates. We conclude from this that rate constants retrieved from angular distributions without additional input information on the relevant interaction potentials are highly unreliable. For the present case of the He^+-Al system the scenario that is consistent with the theoretical input should certainly be favored.

CONCLUSIONS

We have shown that electron spectra arising from grazing incidence He^+-Al(111) collisions are satisfactorily repro-

duced within the rate equation description of the time evolution of the projectile-surface system if theoretical input, which has recently become available in the form of the relevant interaction potentials and transition rate constants, is used. From this we conclude that (1) the theoretical input used is *consistent* with our experimental electron spectra and (2) realistic transition rate constants can be retrieved from measured electron spectra, provided realistic interaction potentials are used in the analysis. We have further explained an apparent discrepancy between the theoretical Auger rate constant used in our analysis and a recently determined semiempirical rate constant.

ACKNOWLEDGMENTS

Fruitful discussions with F. Flores are gratefully acknowledged. This work was performed as part of the program of the ''Stichting voor Fundamenteel Onderzoek der Materie (FOM),'' with financial support from the ''Nederlands Organisatie voor Wetenschappelijk Onderzoek (NOW).''

[1] H. D. Hagstrum, in *Electron and Ion Spectroscopy of Solids*, edited by L. Viermans, J. Vennik, and W. Dekeyzer (Plenum, New York, 1973), p. 273.
[2] A. Niehaus, in *Ionization of Solids by Heavy Particles*, Vol. 306 of *Nato ASI Series B: Physics*, edited by R. A. Baragiola (Plenum Press, New York, 1993), p. 79.
[3] P. A. Zeijlmans van Emmichoven, P. A. A. F. Wouters, and A. Niehaus, Surf. Sci. **195**, 115 (1988).
[4] S. Schippers, S. Oelshig, W. Heiland, L. Folkerts, R. Morgenstern, P. Eeken, I. F. Urazgil'din, and A. Niehaus, Surf. Sci. **257**, 289 (1991).
[5] P. Eeken, J. M. Fluit, I. Urazgil'din, and A. Niehaus, Surf. Sci. **273**, 160 (1992).
[6] H. Brenten, H. Müller, A. Niehaus, and V. Kempter, Surf. Sci. **278**, 183 (1992).
[7] H. Brenten, H. Müller, and V. Kempter, in *Ionization of Solids by Heavy Particles* (Ref. [2]), p. 105.
[8] A. Niehaus, Chem. Phys. **179**, 183 (1994).
[9] W. Heiland, Vacuum **39**, 367 (1989).
[10] J. Merino, N. Lorente, W. More, F. Flores, and M. Yu. Gusev, Nucl. Instrum. Methods Phys. Res. B **125**, 250 (1997).
[11] S. Ossicini, C. M. Bertoni, and P. Gies, Europhys. Lett. **1**, 661 (1986).
[12] F. B. Dunning, P. Nordlander, and G. K. Walters, Phys. Rev. B **44**, 3246 (1991).
[13] N. Lorente and R. Monreal, Surf. Sci. **370**, 324 (1997).
[14] M. A. Cazalilla, N. Lorente, R. Diez Muiño, J.-P. Gauyacq, D. Teillet-Billy, and P. M. Echenique, Phys. Rev. B **58**, 13 991 (1998).
[15] H. Winter, G. Dierkes, A. Hegmann, J. Leuker, H. W. Ortjohann, and R. Zimny, in *Ionization of Solids by Heavy Particles* (Ref. [2]), p. 253.
[16] F. Flores, J. J. Dorado, F. J. Garcia-Vidal, J. Ortega, and R. Monreal, in *Ionization of Solids by Heavy Particles* (Ref. [2]), p. 11.
[17] T. Hecht, H. Winter, and A. G. Borisov, Surf. Sci. **406**, L607 (1998).